Hindawi Publishing Corporation
International Journal of Navigation and Observation
Volume 2010, Article ID 816047, 13 pages
doi:10.1155/2010/816047

*Research Article*

# Nonlinear Modeling of Azimuth Error for 2D Car Navigation Using Parallel Cascade Identification Augmented with Kalman Filtering

**Umar Iqbal,[1,2] Jacques Georgy,[2,3,4] Michael J. Korenberg,[1] and Aboelmagd Noureldin[1,2]**

[1] *Navigation and Instrumentation Research Group (NavINST), Electrical and Computer Engineering Department, Queen's University, ON, Canada K7L 3N6*
[2] *Navigation and Instrumentation Research Group (NavINST), Electrical and Computer Engineering Department, Royal Military College of Canada, ON, Canada K7K 7B4*
[3] *Trusted Positioning Inc., Canada*
[4] *Computer and Systems Engineering Department, Ain Shams University, Egypt*

Correspondence should be addressed to Umar Iqbal, umar.iqbal@queensu.ca

Received 5 May 2010; Revised 3 August 2010; Accepted 23 August 2010

Academic Editor: Gérard Lachapelle



Present land vehicle navigation relies mostly on the Global Positioning System (GPS) that may be interrupted or deteriorated in urban areas. In order to obtain continuous positioning services in all environments, GPS can be integrated with inertial sensors and vehicle odometer using Kalman filtering (KF). For car navigation, low-cost positioning solutions based on MEMS-based inertial sensors are utilized. To further reduce the cost, a reduced inertial sensor system (RISS) consisting of only one gyroscope and speed measurement (obtained from the car odometer) is integrated with GPS. The MEMS-based gyroscope measurement deteriorates over time due to different errors like the bias drift. These errors may lead to large azimuth errors and mitigating the azimuth errors requires robust modeling of both linear and nonlinear effects. Therefore, this paper presents a solution based on Parallel Cascade Identification (PCI) module that models the azimuth errors and is augmented to KF. The proposed augmented KF-PCI method can handle both linear and nonlinear system errors as the linear parts of the errors are modeled inside the KF and the nonlinear and residual parts of the azimuth errors are modeled by PCI. The performance of this method is examined using road test experiments in a land vehicle.

## 1. Introduction

Over the past couple of decades, we are heading towards dense, layered, and complex road systems with increasingly heavy traffic that demands modern navigation systems. We are not able to rely upon GPS systems alone in urban areas where skyscrapers, overpasses, underpasses, and tunnels are familiar attribute of present-day cities as GPS may suffer from outages, interference, jamming, and multipath effects [1–3]. Advanced navigational systems requirements can be fulfilled using complementary navigation methods, relying upon information from motion sensors such as odometers and inertial sensors. These systems are self-contained and hence immune to external interference, but their accuracy deteriorates in the long-term. Deteriorations of performance of these sensors are due to different factors that may include sensor's bias, drift, scale factor instability, and misalignment [4–6]. By integrating the GPS and these motion sensors, a complementary solution can be obtained that is often more accurate than that of independent systems [4]. These sensors are also capable of providing positioning, velocity, and attitude information at higher data rates than GPS. A reliable solution can be achieved during GPS outages using Linearized KF (LKF) and Extended KF (EKF) if high-end navigational and tactical grades inertial navigation systems (INS) are employed. High-end INS may not be used for land navigation due to cost and space limitations.

Micro-Electro-Mechanical Systems-(MEMS)-based inertial sensors have enabled production of lower cost and smaller size inertial measurement units (IMU) with little

power consumption [7]. The complete inertial measurement units (IMUs) are composed of multiple MEMS-based accelerometers and gyroscopes sensors [1]. In order to lower the cost further, recent research [8–10] has explored the applicability of replacing a full IMU with a reduced number of MEMS-based inertial sensors, while still maintaining adequate overall performance. This two-dimensional (2D) reduced inertial sensor system (RISS) computes the vehicle heading and position using low-cost MEMS-based gyroscope integrated with the vehicle odometer exploiting the nonholonomic constraints on land vehicles and integrates these sensors with GPS. This architecture is applied based on the assumption that land vehicle motion is mostly on a plane.

The low-cost MEMS-based sensors have composite error characteristics. Moreover, if linearized system models are utilized for navigation error states estimation with these sensors they can introduce significant errors. These limitations, in turn, may result in suboptimal performance of the integration filter as the assumption of local linearity is violated [11]. This results in a quickly degrading navigation solution provided by KF during GPS outages.

This paper proposes parallel cascade identification (PCI) as a nonlinear system identification technique for modeling the residual azimuth errors (nonlinear parts and all other residuals because of KF mismodeling) after KF prediction of the linear part of these errors. During the availability of the GPS signal, KF continues to operate in the update phase and provides estimates for RISS position, velocity, and attitude errors in a loosely coupled fashion using GPS position and velocity updates. A background routine builds a PCI model for the residual and nonlinear azimuth errors. PCI modeling exploits the nonlinear modeling potential to model all the possible higher order (HO) residual error terms as well as any other residual errors because of mis-modeling in the system model used by KF. When GPS outages occur, KF operates in prediction mode, correcting linear errors based on the system error model, and latest prebuild PCI model provides an estimate of the residual and nonlinear errors to enhance the estimates for azimuth errors. Performance of the proposed augmented KF-PCI scheme is examined by real road-test trajectories and compared with KF solution for a loosely coupled 2D RISS/GPS integration system.

## 2. Mechanization and KF for 2D RISS/GPS Integration

The RISS was suggested [8–10] to have only one single-axis gyroscope with its sensitive axis aligned with the vertical axis of the vehicle. This gyroscope measures the rotation rate in the body frame and compensates for Earth rotation rate along the vertical direction (approximately 15°/hr) around its spin axis and the change of the orientation of the Local level frame with respect to earth before calculating the heading. In [8–10], with the assumption that the vehicle mostly stays in the horizontal plane, the vehicle speed derived from the odometer measurements is used with the heading information obtained from the gyroscope to determine the velocities along the East and North directions, and the whole system is integrated with GPS.

KF is used in this study in a loosely coupled fashion to fuse the RISS computed position and velocity components along the horizontal channels with the corresponding GPS positions and velocities. This enables the computation of the RISS positions, velocities, and azimuth errors as well as the gyroscope and odometer stochastic errors. KF outputs two important variables: the estimated error state vector ($x$) and the error covariance matrix ($P$). The estimated state vector is a vector of RISS positions, velocities, and azimuth errors augmented with the sensors stochastic errors (for both gyroscope and the odometer-derived acceleration). The error covariance matrix is a measure of the estimation uncertainty, which takes into consideration how the sensor noise and dynamic uncertainty contribute to the uncertainty about the estimated error states [11]. By maintaining an estimate of its own estimation uncertainty and the relative uncertainty in the sensor outputs, the KF is able to optimize the estimate to minimize the estimation linear errors. In order for a KF to produce a statistically optimal estimate of its state, the filter's system model equations and measurement model equations matrices must describe exactly the actual dynamical and statistical properties of the system of interest. In the problem at hand, as KF can only estimate the linear errors, nonlinear errors are totally neglected resulting in suboptimal performance.

The error state vector for the proposed RISS includes coordinate errors ($\delta\varphi, \delta\lambda$), velocity errors ($\delta V^e, \delta V^n$), and azimuth error ($\delta A$) as follows:

$$\chi = \begin{pmatrix} \delta\phi & \delta\lambda & \delta V_e & \delta V_n & \delta A & \delta a_{\text{od}} & \delta\omega_z \end{pmatrix}^T, \quad (1)$$

where $\delta a_{\text{od}}$ and $\delta\omega_z$ are the stochastic error in odometer-derived acceleration and the stochastic error in the gyroscope reading, respectively. These errors are passed from one estimate to another with the overall uncertainty in the precision of the estimated quantity drifting with time [12, 13]. Therefore, error models are required for analysis and estimation of different error sources associated with the proposed RISS. Since the errors in dynamic systems are variable in time, they are described by differential equations [11]. Linearization of a nonlinear dynamic system is the most common approach to derive a set of linear differential equations that defines the error states of a dynamic system to be used with KF [14–16]. The time rate of change of RISS position, velocity, and Azimuth errors can be obtained from the following:

$$\begin{pmatrix} \dfrac{d\delta\phi}{dt} \\ \dfrac{d\delta\lambda}{dt} \end{pmatrix} = \begin{pmatrix} o & \dfrac{1}{R_M + h} \\ \dfrac{1}{(R_N + h)\cos\phi} & 0 \end{pmatrix} \begin{pmatrix} \delta V_e \\ \delta V_n \end{pmatrix} + \text{HO}(\delta V_e, \delta V_n, \delta\phi), \quad (2)$$

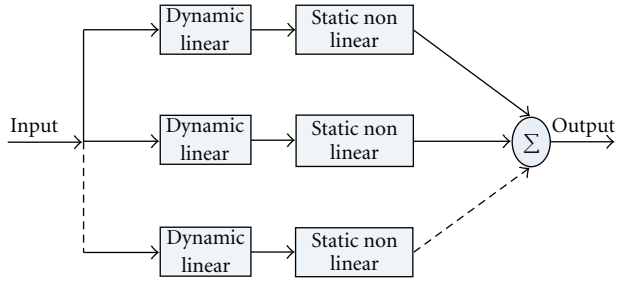


Figure 1: Block diagram of Parallel Cascade Identification.

where $R_M$ and $R_N$ are meridian radius of curvature and normal radius of curvature, respectively,

$$\begin{pmatrix} \frac{d}{dt}(\delta V_e) \\ \frac{d}{dt}(\delta V_n) \end{pmatrix} = \begin{pmatrix} \sin A & a_{\text{od}} \cos A \\ \cos A & -a_{\text{od}} \sin A \end{pmatrix} \begin{pmatrix} \delta a_{\text{od}} \\ \delta A \end{pmatrix} + \text{HO}(\delta a_{\text{od}}, \delta A, \delta \omega_z, \delta V_e, \delta V_n, \delta \phi), \tag{3}$$

where $a_{\text{od}}$ is odometer-derived acceleration,

$$\frac{d}{dt}(\delta A) = -\delta \omega_z + \text{HO}(\delta \omega_z, \delta V_e, \delta \phi). \tag{4}$$

The residual random errors for both the odometer-derived acceleration and the gyroscope are modelled as a first-order Gauss-Markov (GM) process and can be written in form of equation as follows [11, 12]:

$$\begin{pmatrix} \frac{d}{dt}\delta a_{\text{od}} \\ \frac{d}{dt}\delta w_z \end{pmatrix} = \begin{pmatrix} -\gamma_{\text{od}} & 0 \\ 0 & -\beta_z \end{pmatrix} \begin{pmatrix} \delta a_{\text{od}} \\ \delta \omega_z \end{pmatrix} + \begin{pmatrix} \sqrt{2\gamma_{\text{od}}\sigma_{\text{od}}{}^2} \\ \sqrt{2\beta_z\sigma_z{}^2} \end{pmatrix} w(t), \tag{5}$$

where $\beta_z$ is the reciprocal of the correlation time of the random process associated with the gyroscope measurement, $\sigma_z$ is the standard deviation of this random process, and $w(t)$ is unity variance of white Gaussian noise. Similarly $\gamma_{\text{od}}$ is the reciprocal of the correlation time of the random process associated with the speedometer's acceleration and $\sigma_{\text{od}}$ is the standard deviation of this random process. The necessity of accurate stochastic modeling is not fulfilled particularly in case of low-cost MEMS-based sensors when sensor stochastic errors are modeled as 1st order GM.

While it showed adequate performance with higher grades of inertial sensors, KF with its linearized model and GM model for sensor errors is not able to handle higher order terms when using low-cost MEMS-based inertial sensors; this will affect the performance of the solution during GPS outages. To achieve reliable navigation, a nonlinear system identification technique is required to establish a more reliable azimuth error model, which not only can handle higher order errors, but can also tolerate complex stochastic errors and any other residual errors not well modeled by KF. The focus here is on azimuth since it is the major source of error in the RISS system that contributes to position and velocity errors. Parallel Cascade Identification, a nonlinear modeling technique, is used to augment KF in order to overcome its limitations and enhance the accuracy of MEMS-grade RISS solutions.

## 3. Parallel Cascade Identification

System identification is an effort to infer the dynamic operator between system input and output from an analysis of time-varying input-output data. Most techniques assume linearity due to the simplicity of analysis as nonlinear system techniques make analysis much more complicated and difficult than for the linear case. However, for more realistic dynamic characterization, nonlinear system techniques are suggested. Parallel cascade identification (PCI) is a nonlinear system identification technique proposed by Korenberg [17]. This technique models the input/output behaviour of a nonlinear system by a sum of parallel cascades of alternating dynamic linear (L) and static nonlinear (N) elements. The parallel array shown in Figure 1 can be built up one cascade at a time [18].

Palm [19] proved that any discrete-time Volterra series with finite memory and anticipation can be uniformly approximated by a finite sum of parallel LNL cascades, where the static nonlinearities N are exponentials and logarithmic functions. Korenberg [18] showed that any discrete-time doubly finite (finite memory and order) Volterra series can be exactly represented by a finite sum of LN cascades where the N are polynomials. A key advantage of this technique is that it is not dependent on a white or Gaussian input, but the identified individual L and N elements may vary depending on the statistical properties of the input chosen [18]. The cascades can be found one at a time and nonlinearities in the models are localized in static functions. This reduces the computation as higher order nonlinearities are approximated using higher degree polynomials in the cascades rather than higher order kernels in a Volterra series approximation.

The method begins by approximating the nonlinear system by a first such cascade. The residual (i.e., the difference between the system output and the cascade outputs) is treated as the output of a new nonlinear system, and a second cascade is found to approximate the latter system, and thus the parallel array can be built up one cascade at a

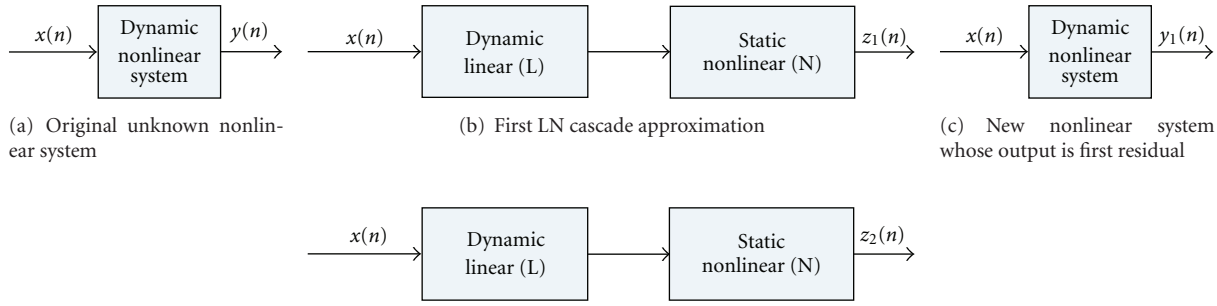


(a) Original unknown nonlinear system

(b) First LN cascade approximation

(c) New nonlinear system whose output is first residual

(d) Second LN cascade

Figure 2: Idea of PCI algorithm.

time. Having an unknown dynamic nonlinear system with accessible input $x(n)$ and output $y(n)$ (where $n = 0, \ldots, T$), one can model it using a parallel cascade supposing that the output can depend on delayed input values $x(n - j)$, for $j = 0, \ldots, R$, and that the maximum degree of nonlinearity required for good approximation of the system is "$D$". PCI algorithm can be explained briefly in the following steps:

(1) Approximate the dynamic nonlinear system by a first cascade of a dynamic linear (L) followed by a static nonlinear (N) element as in Figure 2(b). The first cascade output is $z_1(n)$.

(2) Compute first residual $y_1(n) = y(n) - z_1(n)$.

(3) Approximate the new nonlinear system having input $x(n)$ and output $y_1(n)$ by a cascade of $L_2$ followed by $N_2$ as in Figure 2(d).

(4) Compute second residual $y_2(n) = y(n) - z_2(n)$.

(5) And so on ...

Let $y_k(n)$ be the residual after fitting the $k$th cascade, so $y_o(n) = y(n)$. Let $z_k(n)$ be the output of the $k$-th cascade, so

$$y_k(n) = y_{k-1}(n) - z_k(n), \quad \text{where } k = 1, 2, \ldots. \tag{6}$$

When identifying the $k$th cascade, the current residual before the addition of the $k$th cascade is $y_{k-1}(n)$. The method employed in this research to get the impulse response of the linear element $L_k$ at beginning the $k$-th cascade uses cross-correlations of the input with the current residual:

(a) Input residual cross-correlation

$$\varphi_{xy_{k-1}}(j) = \frac{1}{(T - R + 1)} \sum_{n=R}^{T} y_{k-1}(n)x(n - j), \quad j = 0, \ldots, R. \tag{b}$$

$\varphi_{xxy_{k-1}}(j, A) \pm c\delta(j - A)$, where the sign is chosen at random, $A$ is chosen at random from $0, \ldots, R$, and $c$ is chosen such that $c \to 0$ as $\overline{y_{k-1}^2(n)} \to 0$, for example, $c = \overline{y_{k-1}^2(n)}/\overline{y^2(n)}$ (here the overbar means the finite-time average from $n = R$ to $n = T$ as in the expression for $\varphi_{xy_{k-1}}(j)$ immediately above).

(c) $\varphi_{xxxy_{k-1}}(j, A_1, A_2) \pm c_1\delta(j - A_1) \pm c_2\delta(j - A_2)$.

(d) We can use expression up until $\varphi_{x\ldots xy_{k-1}}(j, A_1, \ldots, A_{D-1}) \pm c_1\delta(j - A_1) \pm \cdots \pm c_{D-1}\delta(j - A_{D-1})$ but in practice third order is typically enough.

The output of the linear element is calculated by convolution summation as follows:

$$u_k(n) = \sum_{j=0}^{R} g_k(j)x(n - j), \tag{7}$$

where the linear element's output $u_k(n)$ depends on input values $x(nj), x(nj-1), \ldots x(nj-R)$ so the memory length of the linear element is $R + 1$, and $g_k(j)$ is the impulse response of the linear element $L_k$ at beginning the $k$th cascade.

Usually for computation purposes, the following is done before the polynomial fitting. First $\overline{u_i^2(n)}$ is calculated, let it equals $M$. Then the impulse response of the dynamic linear element is adjusted to be $\widetilde{g}_i(j) = g_i(j)/\sqrt{M}$, this ensures that $\overline{u_i^2(n)} = 1$.

Best fitting of current residual can be used to find the polynomial coefficients of the static nonlinearities. The $D+1$ coefficients "$a_{\mathrm{id}}$" of the polynomial static nonlinearity that follows the linear element, that is best fit to minimize the MSE of the approximation, are found as follows:

$$\begin{aligned} e_i &= \overline{\left( y_{i-1}(n) - \sum_{d=0}^{D} a_{\mathrm{id}} u_i^d(n) \right)^2} \\ &= \frac{1}{T - R + 1} \sum_{n=R}^{T} \left( y_{i-1}(n) - \sum_{d=0}^{D} a_{\mathrm{id}} u_i^d(n) \right)^2. \end{aligned} \tag{8}$$

As noted, the overbar here means finite-time average. This leads to $D + 1$ equation in $D + 1$ unknowns "$a_{\mathrm{id}}$"

$$\overline{y_{i-1}(n)u_i^q(n)} = \sum_{d=0}^{D} a_{\mathrm{id}} \overline{u_i^{d+q}(n)}, \quad \text{where } q = 0, \ldots, D. \tag{9}$$

These resulting cascades are such as to drive the cross correlations of the input with the residual to zero [18, 20]. A threshold based on a standard correlation test for determining whether a cascade's reduction of the mean

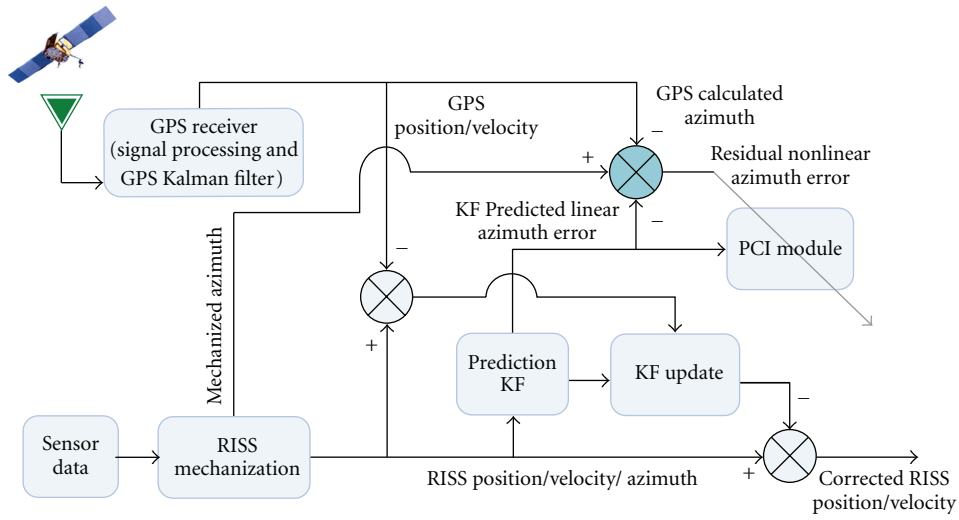


Figure 3: Augmented KF/PCI method during GPS availability.

square error (MSE) justifies its addition to the model is as follows:

$$\overline{z_k^2(n)} > \frac{4}{T-R+1}\overline{y_{k-1}^2(n)}. \tag{10}$$

In (10), $\overline{z_k^2(n)}$ denotes the mean square of the candidate cascade's output, and $\overline{y_{k-1}^2(n)}$ denotes the mean square of the current residual; that is, the residual remaining from the cascades already presents in the model.

According to [18], the process of building a parallel cascade can have one of the following stopping conditions:

(1) When a certain number of cascades is added.

(2) When a certain number of cascades is tested (either added or not).

(3) When the MSE is sufficiently small.

(4) When no remaining candidate cascade can reduce the MSE more than a small threshold level.

## 4. Augmenting KF with PCI to Model the Residual and Nonlinear Azimuth Errors

In order to apply PCI to RISS/GPS integration, this research proposes a KF-PCI method where the role of PCI is to model the residual azimuth error not modeled by KF; this includes nonlinear parts as well as other residuals due to mismodeling, while the linear parts of the errors are modeled inside the KF. When GPS is available, KF is utilized to perform RISS/GPS integration. For the KF, its input and output are the same as what is known traditionally, except that the prediction phase output is also provided to the outside world not just the final output of the update phase (when measurement update is available). When GPS is available, the KF outputs both the outcome of the update phase (to be the positioning solution given to the user) and the outcome of the prediction phase (to be used by PCI in its building phase). In parallel, during GPS availability, as a background routine, the PCI algorithm runs to build a model for the residual azimuth errors. The PCI algorithm building the model needs an input and a target output. The input is the azimuth error coming out of the KF prediction phase (i.e., the linear part modeld by KF system model). The output consists of all the residuals not modeled by KF (because of linearization, mis-modeling of 1st order GM, and other approximations). The prediction of KF azimuth ($\delta A_{\overline{KF}}$) is used together with mechanization results $A_{\text{Mech}}$ *and* GPS aiding azimuth $A_{\text{GPS}}$ to derive the true nonlinear residual error of azimuth $\triangle A_R$ that was not modeled by the KF system model. During GPS availability and when the vehicle is in motion, the azimuth calculated from GPS is obtained as follows:

$$A_{\text{GPS}} = \tan^{-1}\left(\frac{V_e^{\text{GPS}}}{V_n^{\text{GPS}}}\right). \tag{11}$$

The residual azimuth error $\Delta A_R$ is given as follows:

$$\Delta A_R = A_{\text{Mech}} - \delta A_{\overline{\text{KF}}} - A_{\text{GPS}}. \tag{12}$$

The schematic diagram that shows RISS/GPS integration and includes the building of a PCI model for the residual azimuth errors is shown in Figure 3. As the training data, $\triangle A_R$ provides the reference output to build the PCI model of the azimuth residual nonlinear error. Moreover, the Azimuth predictions from KF are sent to PCI as the input to construct the model. Dynamic characteristics between system input and output help to identify the nonlinear and residual errors, and the algorithm can then build a residual nonlinear azimuth error model.

When less than four satellites are visible, a GPS outage occurs as a loosely coupled architecture is used. When there is

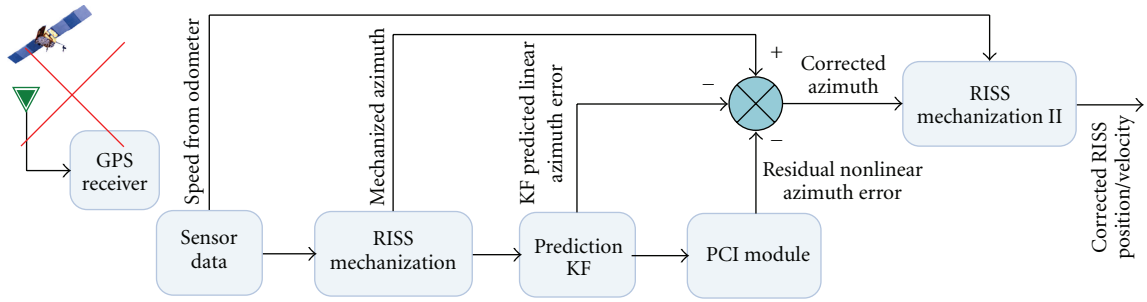


Figure 4: Augmented KF/PCI method during the GPS outage.

Table 1: Crossbow IMU specifications [21].

| Size | $7.62 \times 9.53 \times 3.2$ (cm) | Input voltage | 9–30 V dc |
|---|---|---|---|
| Weight | 0.59 kg | Power | <3 W |
| Max data rate | 200 Hz | Connector | RS-232 |
| Start-up time | <1 s | Input voltage | 9–30 V dc |
| Accelerometer | | Gyroscope | |
| Range | ± 2 g | Range | ± 100 g |
| Bias | ± 30 mg | Bias | < ± 2.0 deg/sec |
| Scale factor | <1% | Scale factor | < 1 % |
| Random walk | <0.15 m/s/$\sqrt{hr}$ | Random walk | <2.25 deg/$\sqrt{hr}$ |
| | | Linearity | <1% |

a GPS outage, the KF outputs the outcome of the prediction phase to be used as input for the identified parallel cascade model in its running phase. This identified model is used to predict the residual and nonlinear azimuth errors from the KF prediction for the linear azimuth error. The prebuilt nonlinear model predicts the azimuth residual error $\Delta A_R$ from the KF prediction for the linear part of this error $\delta A_{\text{KF}}^{-}$, thus the corrected azimuth $A_{\text{Corrected}}$ can then be obtained as

$$A_{\text{Corrected}} = A_{\text{Mech}} - \delta A_{\text{KF}}^{-} - \Delta A_R. \tag{13}$$

The corrected azimuth angle is passed to a new standalone RISS mechanization shown in Figure 4 (labelled RISS Mechanization II) to calculate corrected position and velocity. As a result, this architecture derives more accurate position $P_{\text{Corrected}}$ and velocities $V_{\text{Corrected}}$ during GPS outages; this is the provided navigation solution in case of GPS outages.

## 5. Experimental Setup and Results

The performance of the developed navigation solution was examined with road test experiments in a land vehicle. The experimental data collection was carried out using a full-size passenger van carrying a suite of measurement equipment that included inertial sensors, GPS receivers, antennae, and computers to control the instruments and acquire the data. Two low-cost gyroscopes were used in this work, one was from the MEMS-grade IMU made by Crossbow whose model is IMU300CC-100. The specifications of this IMU are in Table 1, and the detailed specifications can be found in [21]. The other was an ultra-low-cost IMU that utilizes MEMS sensors from Analog Devices Inc. (ADI). The specifications of this IMU are in Table 2 and the detailed specifications can be found in [22, 23]. The vehicle's forward speed readings were obtained through vehicle builtin sensors through on-board diagnostics version II (OBD II) interface using a device called CarChip. The specifications of this device are described in [24], and more details about OBD II speed readings can be found in [25]. The sample rate for the collection of speed readings was 1 Hz. To demonstrate the performance of the proposed solution, two GPS receivers were used in the presented results: one was a low-cost Trimble Lassen SQ GPS receiver [26] and the other was the NovAtel OEM4 [27]. The results were evaluated with respect to a reference solution made by NovAtel, where Honeywell HG1700 tactical grade IMU [28] was integrated with the NovAtel OEM4 GPS receiver. Together the NovAtel and Honeywell systems were integrated with an off the shelf unit developed by NovAtel, the G2 ProPack SPAN unit [29]. The NovAtel system provided the reference solution to validate the proposed method and to examine the overall performance during natural or simulated GPS outages.

Several road test trajectories were carried out using the setup described above. The sensors data were collected during the road tests and the navigation solutions were run offline in post processing using the logged data. Three trajectories will be presented in this paper to show the performance of the proposed KF-PCI method in environments encompassing several different conditions.

Table 2: ADI IMU specifications [22, 23].

| Specifications | Gyroscope | |
|---|---|---|
| | Before lab calibration | After lab calibration |
| Range | ± 150 deg/s | ± 150 deg/s |
| Bias | < ± 24 deg/s | < ± 0.5 deg/s |
| Bias instability | 40 deg/hr (100s) | 40 deg/hr (100s) |
| Scale factor | 10% | 0.1% |
| Angle random walk | 3 deg/$\sqrt{hr}$ | 3 deg/$\sqrt{hr}$ |
| Nonlinearity | 0.1% | 0.1% |
| Axis misalignment | ± 1 deg | ± 0.2 deg |
| Specifications | Accelerometer | |
| | Before lab calibration | After lab calibration |
| Range | ± 5 g | ± 5 g |
| Bias | < ± 2500 mg | < ± 6 mg |
| Bias instability | 0.2 mg (100s) | 0.2 mg (100s) |
| Scale factor | 10% | 0.1% |
| Velocity random walk | 0.135–0.195 m/s/$\sqrt{hr}$ | 0.135–0.195 m/s/$\sqrt{hr}$ |
| Nonlinearity | 0.2% | 0.2% |
| Axis misalignment | ± 1 deg | ± 0.2 deg |

*5.1. First Trajectory.* The first road test trajectory considered for these results was in Kingston, Ontario, Canada. This road test was performed for nearly 35 minutes of continuous vehicle navigation and a distance of around 23 km. The ultimate check for the proposed system's accuracy was during GPS signal blockage, which was intentionally introduced in post processing. Ten simulated GPS outages of 60-second each for the first case (shown as dotted black circles overlaid on the map in Figure 5) and 120-second each for the second case (shown as big blue circles overlaid on the map in Figure 5) were introduced such that they encompass different conditions, including straight portions, turns, high speeds, slow speeds, and stops. Sensors used for this trajectory were the ultra-low-cost ADI IMU and the low-cost Trimble Lassen SQ GPS receiver. The errors estimated by KF-PCI and KF-only solutions were evaluated with respect to the NovAtel reference solution.

*5.1.1. Analysis of First Trajectory for 60 Seconds of GPS Outages.* The results of KF-PCI method and KF-only solution for RISS/GPS integration are presented in Figures 6 and 7 for 60-second outages. The prior shows the root mean square (RMS) error and the later shows the maximum error in the estimated position during the ten simulated GPS outages for the two used techniques. Overall performance improvement using KF-PCI method was 69.91% for 10 simulated 60-second GPS outages as KF-PCI method is able to model and suppress the nonlinear and the residual errors in the azimuth, which could not be handled by the linearized error models of KF-only solution for RISS/GPS integration and its linear GM model.

*5.1.2. Analysis of First Trajectory for 120 Seconds of GPS Outages.* In this run, The trajectory was more challenging because the duration of the ten simulated GPS outages was increased to 120-second instead of 60-second. Figures 8 and 9 show the Maximum and RMS positional error for 120-second GPS outages.

During GPS outages, the KF-PCI method is able to improve the overall positioning performance by 85.85% over the KF solution for 120-second outages. This is due to the fact that error in position depends on many factors such as outage duration, azimuth error, and vehicle velocities. The position errors in this run with 120-second outages are higher than those in the case with 60-second outrages, especially in the KF-only solution. Thus the enhancement of KF-PCI over KF-only is higher in the 120-second case than that in the 60-second case.

Figure 10 shows the Azimuth error during the GPS outages of 120-second for both KF-PCI method and KF-only method. It is evident that, as the trajectory progressed, the effect of azimuth errors becomes more dominant in the KF-only solution. The uncompensated gyroscope drift that grows with time, the nonlinear terms that were not modeled by KF, and the other residual errors due to mismodelling combine together and cause this error to increase considerably. On the other hand, KF-PCI method is able to model and suppress the nonlinear azimuth error and the other residual errors that were not modeled by KF.

To examine the performance of the proposed method during long outages of 120-second and impact of the vehicle dynamics on the navigational solution, the 5th and 9th GPS outages are considered. During the 5th outage (Figure 11), the vehicle was going on a curved road at a speed of 45 km/h followed by a sharp turn, where it decelerated to 2 km/h speed. The vehicle accelerated again to a speed of 45 km/h with some deviation in the speed near another turn as shown in Figure 12. The maximum position error for KF-PCI method is 16.96 meters and for KF is 208.9 meters. The 9th outage (Figure 13) was during two consecutive turns and


Figure 5: Road Test Trajectory in Kingston. Dotted black circles show 60-second GPS outages and big blue circles show 120-second GPS outages.

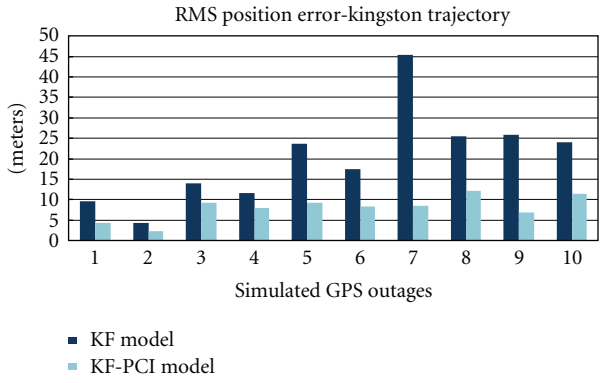


Figure 6: RMS position error during 60-second GPS outages.

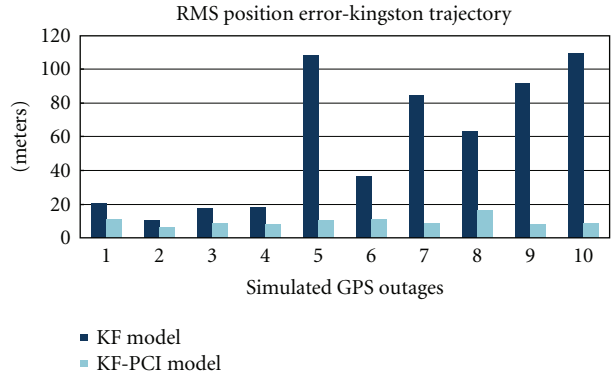


Figure 8: RMS position error during 120-second GPS outages.

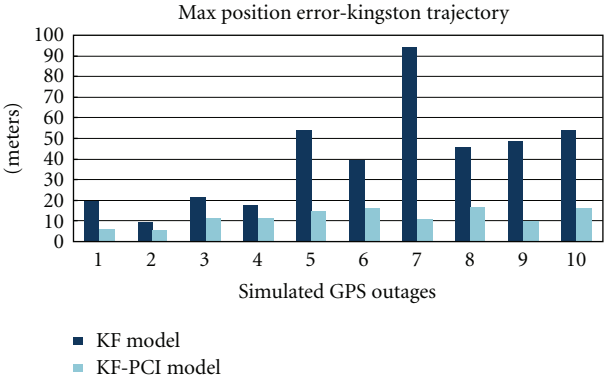


Figure 7: Max. Position error during 60-second GPS outages.

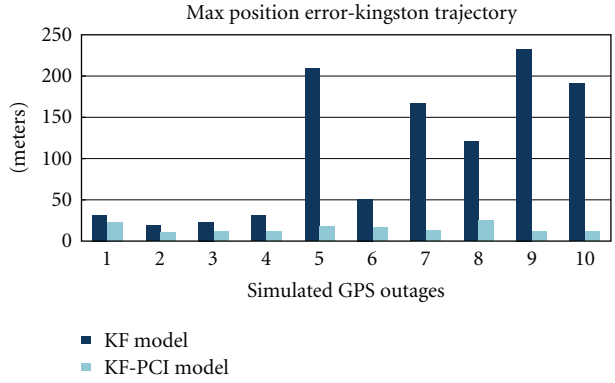


Figure 9: Max. Position error during 120-second GPS outages.

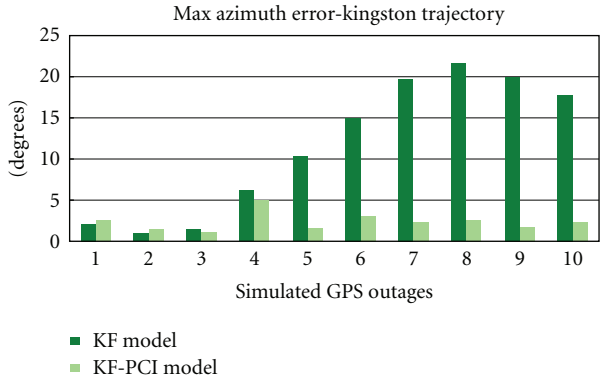


Figure 10: Max. Azimuth Error during 120-second GPS outages.

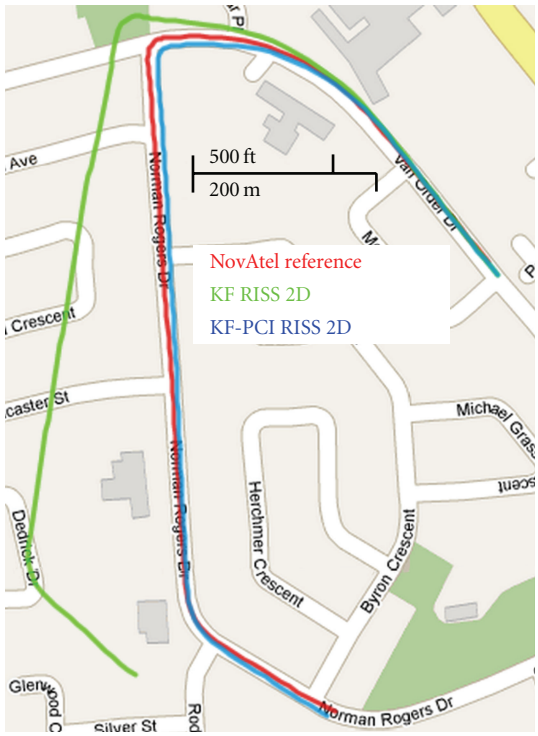


Figure 11: Performance during GPS outage no. 5.

a combination of sharp deceleration and then acceleration of the vehicle. Initial speed was about 40 km/h at the start of outage and on the first turn reduced to 6 km/h. Then sharp acceleration from 6 km/h to 30 km/h was observed. But again speed reduced to 5 km/h at the second turn and the vehicle accelerated to 40 km/h as shown in Figure 14. The maximum position error for KF-PCI method is 11.7 meters and for KF is 231.5 meters. Outages 5th and 9th clearly show the superior performance of KF-PCI method over KF solution. KF-PCI method remained successful in mitigating the nonlinear and the other residual errors in azimuth and it was less affected by increasing the duration of the outages, on the other hand the error in KF solution increased significantly with the increase in duration.

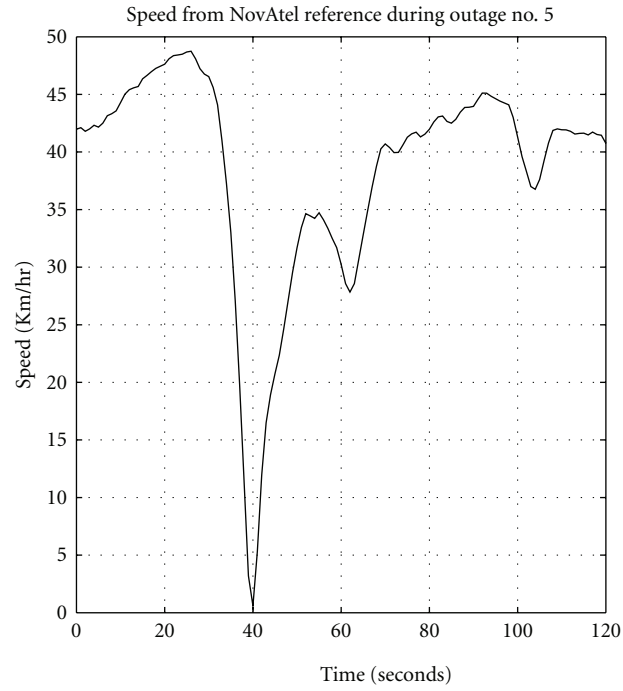


(a)

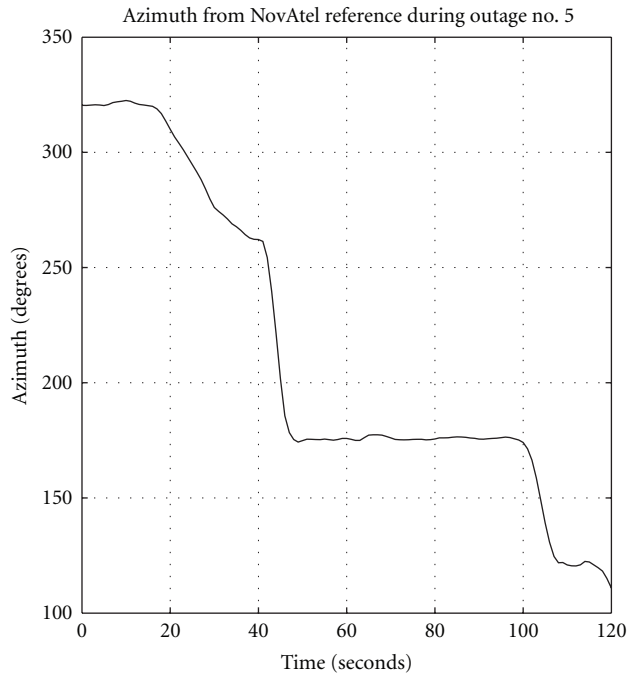


(b)

Figure 12: Speed at top and Azimuth at bottom during GPS outage no. 5.

*5.2. Second Trajectory.* The second road test trajectory (Figure 15) was in Montreal, Quebec, Canada. This road test was performed for nearly 120 minutes of continuous vehicle navigation and a distance of around 37 km. This trajectory was in a downtown scenario with urban canyons in some parts; it had several natural GPS outages. The sensors used

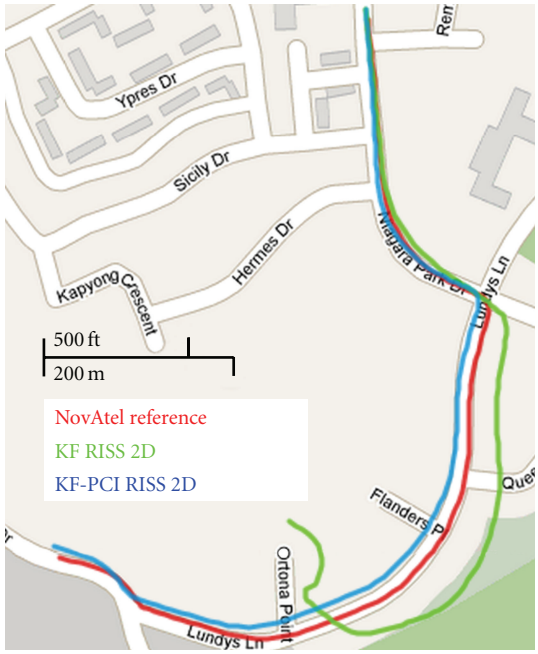


Figure 13: Performance during GPS outage no. 9.

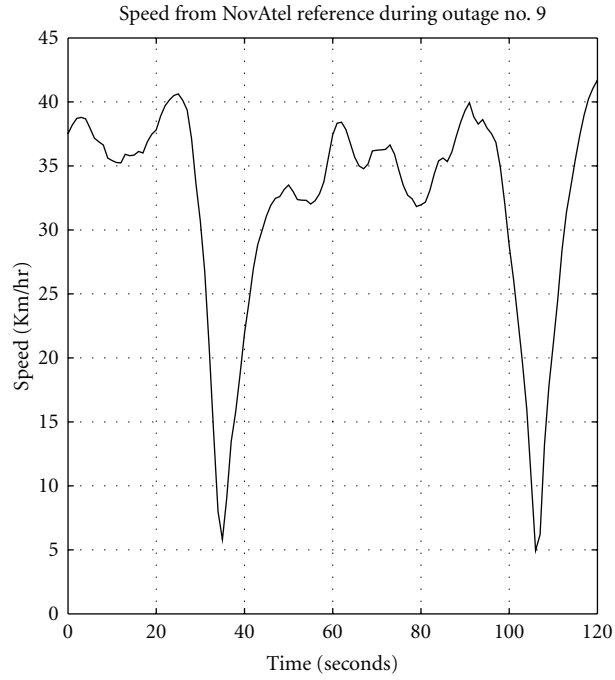


(a)

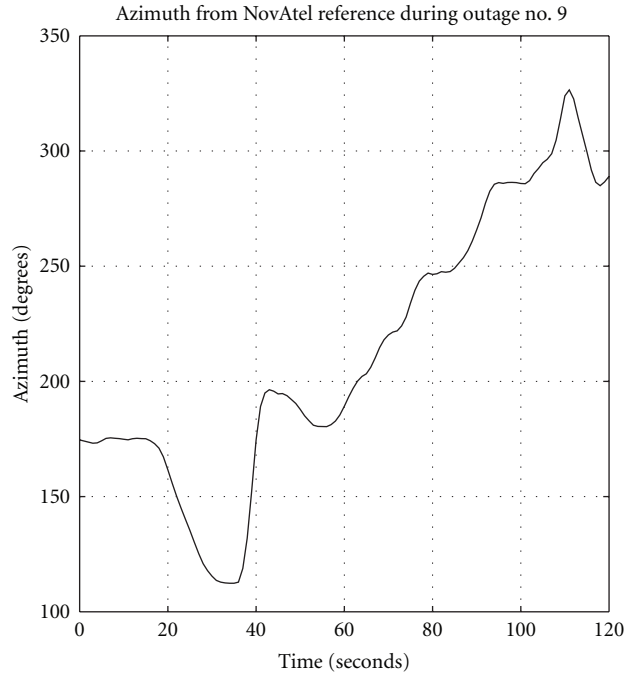


(b)

Figure 14: Speed at top and Azimuth at bottom during GPS outage no. 9.

for this trajectory were Crossbow IMU and NovAtel OEM4 GPS receiver. In order to reduce the number of outages presented and to examine the system performance in longer outages, the adjacent natural outages were combined into longer outages with different durations. The number of the grouped natural outages is seven. Furthermore, three simulated outages are introduced, to be more specific they are the first three outages. The ten outages are shown as circles overlaid on the map in Figure 15, and their durations are shown in Table 3. These outages encompass straight portions, turns, and frequent stops.

Figure 16 compares the maximum values of the position errors for KF and KF-PCI methods for the ten GPS outages of different durations. The overall improvement in performance is 63.46% using the proposed KF-PCI technique as compared to the KF-only technique. It is observed that during periods of long GPS outages, adequate improvement in positioning accuracy has been obtained using the KF-PCI method.

*5.3. Third Trajectory.* The third road test trajectory considered for this paper was performed in the city of Kingston, Ontario, Canada, as shown in Figure 17. This road test was performed for nearly 48 minutes of continuous vehicle navigation and a distance of around 22 km. The check for the proposed system's performance in this trajectory is presented in a way to show how long KF and KF-PCI can bridge the GPS gap keeping 5 meter accuracy for both the RMS and maximum positional errors. Ten GPS outages of 60-second duration were introduced in post processing such that they encompass different conditions including straight portions, turns, different speeds, and stops. The locations of outages are shown as circles overlaid on the map in Figure 17. The errors in the estimated solutions are evaluated with respect to the NovAtel reference solution. The sensors used for this trajectory were Crossbow IMU and low-cost Trimble Lassen SQ GPS receiver.

The results of KF-PCI method and KF-only solution for RISS/GPS integration are presented in Figures 18 and 19. For

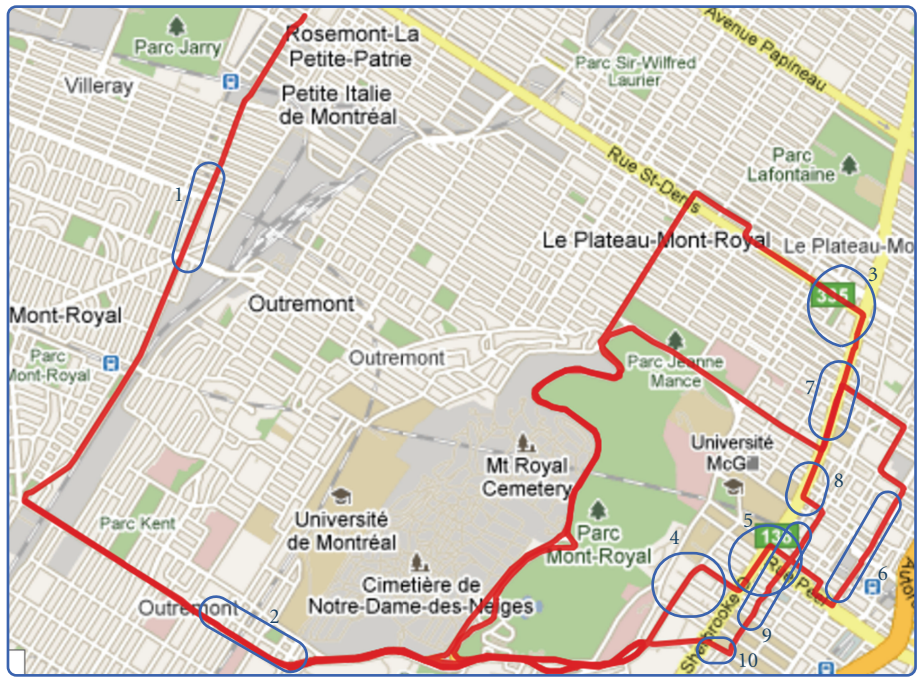


Figure 15: Road Test Trajectory in Montreal including downtown area. Circles indicate the locations of GPS outages.

Table 3: Duration of outages in Montreal Trajectory.

| Outage No. | 1 | 2 | 3 | 4 | 5 | 6 | 7 | 8 | 9 | 10 |
|---|---|---|---|---|---|---|---|---|---|---|
| Duration (Sec) | 180 | 180 | 180 | 120 | 170 | 120 | 155 | 180 | 230 | 50 |

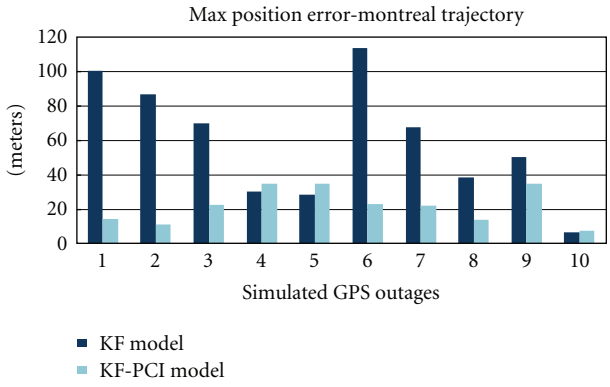


Figure 16: Max. Position error during GPS outages.

the ten simulated GPS outages and the two used techniques, these figures show the duration of time in seconds until RMS positional error and maximum positional error reached 5 meters or 60 seconds (if the 5 m error was never reached during this duration).

It is evident from both graphs that the proposed KF-PCI solution provides better results than KF-only solution for all outages. Overall improvement in the duration before the RMS and maximum positional error reaches 5 m is 86.74% and 87.93%, respectively, when using the proposed KF-PCI technique as compared to KF-only solution. The best performance was observed during the 4th outage where maximum positional error for KF-PCI remained with 5 meter error range for the whole outage duration of 60 seconds whereas KF-only solution crossed the threshold of 5 meter just after 5 seconds.

## 6. Conclusion

This paper proposed a KF-PCI method to curtail both linear and nonlinear errors in azimuth of MEMS-grade gyroscope for 2D RISS integrated with GPS using loosely coupled integration approach. Error growth of positioning solutions employing low-cost MEMS-grade sensors is incredibly swift. KF with its linearized models and GM model for sensor errors is not able to handle these low-cost sensors in the same quality, it was able to handle the higher grades of inertial sensors. PCI is able the handle nonlinear, nonstationary azimuth errors as well as the stochastic sensor errors of the gyroscope; these are the principal cause of positional error growth particularly during the long outages when using low-cost sensors. A PCI model of all the residual azimuth errors is built during the availability of GPS, and as an outage occurs the prebuilt PCI model starts to compensate for the nonlinear and other residual azimuth errors. This method is able to handle linear part of the errors by KF and nonlinear


Figure 17: Road Test Trajectory from downtown Kingston. Circles indicate the locations of GPS outages.

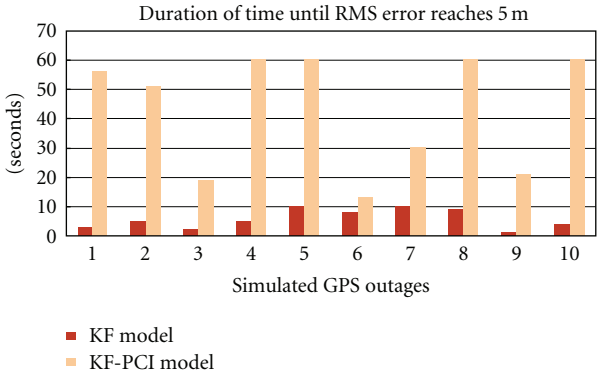


Figure 18: Duration of time in sec. until RMS positional error reaches 5 m during outages.

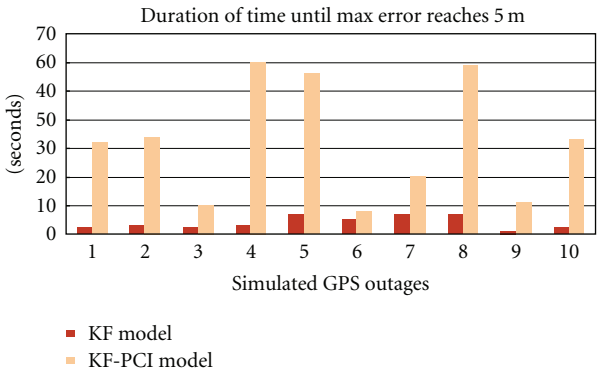


Figure 19: Duration of time in sec. until Max. Positional error reaches 5 m during outages.

and residual parts that were not modeled by KF, which becomes especially significant when MEMS- grade sensors are used.

The proposed KF-PCI navigation solution was tested with real road-test trajectories using different sensors and compared to KF-only solution. The results of three trajectories were presented. The first trajectory was in downtown Kingston comprising urban streets, where the road test vehicle experienced motion dynamics of a typical urban trip with frequent stops. The sensors used for this trajectory were the ultra-low-cost ADI IMU and the low-cost Trimble Lassen SQ GPS receiver. This trajectory was tested for 10 simulated GPS outages once with 60-second and once with 120-second duration to examine the effectiveness of the proposed technique. The KF-PCI solution surpasses KF solution; the overall performance improvement in maximum position error was 69.91% for the 60-second GPS outages, and it was amplified to 85.85% for 120-second outages. The second trajectory presented was in Montreal and it contained ten GPS outages with a mix of grouped natural and simulated outages. The sensors used for this trajectory were the Crossbow IMU and the NovAtel OEM4 GPS receiver, and the overall performance improvement was 63.46%. The last trajectory presented was in Kingston area on a different route with Crossbow IMU and Trimble Lassen SQ GPS receiver. The performance was tested in terms of the duration of time in seconds until the RMS positional error and maximum positional error reached 5 meters or 60 seconds (which is the simulated outages duration). The overall improvement in duration for the maximum position error case was 87.93% using proposed KF-PCI technique as compared to that of the KF-only solution.

During GPS outages, the KF-PCI module can correct the residual and nonlinear azimuth errors and outperforms the traditional KF-only solution especially during long-term GPS outages. Results positively demonstrate the utilization of KF-PCI method as a data fusion technique for the low cost MEMS-grade 2D RISS/GPS integration for car navigation.

## References

[1] M. S. Grewal, L. R. Weill, and A. P. Andrews, *Global Positioning Systems, Inertial Navigation, and Integration*, Wiley-Interscience, New York, NY, USA, 2nd edition, 2007.

[2] J. A. Farrell, *The Global Positioning System & Inertial Navigation*, McGraw–Hill, New York, NY, USA, 1998.

[3] A. El-Rabbany, *Introduction to GPS—The Global Positioning System*, Artech House, Norwood, Mass, USA, 2002.

[4] R. V. C. Wong, K. P. Schwarz, and M. E. Cannon, "High-accuracy kinematic positioning by GPS-INS," *Navigation, Journal of the Institute of Navigation*, vol. 35, no. 2, pp. 275–287, 1988.

[5] A. Noureldin, *EE523: Course Notes on Mobile Multi-Sensor Systems Integration*, Royal Military College of Canada, Kingston, Canada, 2007.

[6] A. Noureldin, T. B. Karamat, M. D. Eberts, and A. El-Shafie, "Performance enhancement of MEMS-based INS/GPS integration for low-cost navigation applications," *IEEE Transactions on Vehicular Technology*, vol. 58, no. 3, pp. 1077–1096, 2009.

[7] K. Sheard, I. Scaysbrook, and D. Cox, "MEMS sensor and integrated navigation technology for precision guidance," in *Proceedings of the IEEE/ION Position, Location, and Navigation Symposium (PLANS '08)*, pp. 1145–1151, Monterey, Calif, USA.

[8] U. Iqbal, A. F. Okou, and A. Noureldin, "An integrated reduced inertial sensor system—RISS/GPS for land vehicle," in *Proceedings of the IEEE/ION Position, Location, and Navigation Symposium (PLANS '08)*, pp. 912–922, Monterey, Calif, USA.

[9] U. Iqbal and A. Noureldin, *Integrated Reduced Inertial Sensor System/GPS for Vehicle Navigation*, VDM, Saarbrücken, Germany, 2009.

[10] U. Iqbal, T. B. Karamat, A. F. Okou, and A. Noureldin, "Experimental results on an integrated GPS and multisensor system for land vehicle positioning," *International Journal of Navigation and Observation*, vol. 2009, Article ID 765010, 18 pages, 2009.

[11] A. Gelb, *Applied Optimal Estimation*, MIT Press, Cambridge, UK, 1974.

[12] R. G. Brown and P. Y. C. Hwang, *Introduction to random signals and applied Kalman filtering*, John Wiley & Sons, New York, NY, USA, 1997.

[13] G. Welch and G. Bishop, *An Introduction to the Kalman Filter*, ACM, Rockville, Md, USA, 2001.

[14] K. P. Schwarz and M. Wei, "A framework for modelling kinematic measurements in gravity field applications," *Bulletin Géodésique*, vol. 64, no. 4, pp. 331–346, 1990.

[15] D. H. Titterton and J. L. Weston, *Strapdown Inertial Navigation Technology*, Peregrinus, London, UK, 1997.

[16] M. Wei and K. P. Schwarz, "A Strapdown inertial algorithm using an earth-fixed cartesian frame," *Navigation, Journal of the Institute of Navigation*, vol. 37, no. 2, pp. 153–167, 1990.

[17] M. J. Korenberg, "Statistical identification of parallel cascades of linear and nonlinear systems," in *Proceedings of the 6th IFAC Symposium on Identification and System Parameter Estimation*, vol. 1, pp. 580–585, 1982.

[18] M. J. Korenberg, "Parallel cascade identification and Kernel estimation for nonlinear systems," *Annals of Biomedical Engineering*, vol. 19, no. 4, pp. 429–455, 1991.

[19] G. Palm, "On representation and approximation of nonlinear systems. Part II: discrete time," *Biological Cybernetics*, vol. 34, no. 1, pp. 49–52, 1979.

[20] J. M. Eklund and M. J. Korenberg, "Simulation of aircraft pilot flight controls using nonlinear system identification," *Simulation*, vol. 75, no. 2, pp. 72–81, 2000.

[21] IMU300—6DOF Inertial Measurement Unit: Crossbow Technology Inc., San Jose, CA.

[22] X. Niu and N. El-Sheimy, "Development of a low-cost MEMS IMU/GPS navigation system for land vehicles using auxiliary velocity updates in the body frame," in *Proceedings of the 18th International Technical Meeting of the Satellite Division of the Institute of Navigation (ION GNSS '05)*, Long Beach, Calif, USA, 2005.

[23] X. Niu, C. Goodall, S. Nassar, and N. El-Sheimy, "An efficient method for evaluating the performance of MEMS IMUs," in *Proceedings of the IEEE/ION Position, Location, and Navigation Symposium (PLANS '06)*, pp. 766–771, San Diego, Calif, USA, 2006.

[24] CarChip OBDII-Based Vehicle Data Logger and Software: Davis Instruments, http://www.davisnet.com/product_documents/drive/spec_sheets/8226_Specs_CarChipPsheets/8226_Specs_CarChipP.

[25] J. Wilson, "Low-cost PND dead reckoning using automotive diagnostic links," in *Proceedings of the 20th International Technical Meeting of the Satellite Division of the Institute of Navigation (ION GNSS '07)*, pp. 2066–2074, Fort Worth, Tex, USA, 2007.

[26] Lassen SQ GPS Receiver—System Designer Reference Manual: Trimble Navigation Limited, http://trl.trimble.com/docushare/dsweb/Get/Document-138833/LassenSQ_0601print.pdf.

[27] OEM4-G2, http://www.novatel.ca/Documents/Papers/oem4g2.pdf.

[28] HG1700 Inertial Measurement Unit: Honeywell, http://www51.honeywell.com/aero/common/documents/myaerospacecatalog-documents/Missiles-Munitions/HG1700_Inertial_Measurement_Unit.pdf .

[29] SPAN Technology System User Manual OM-20000062: NovAtel Inc., www.novatel.com/Documents/Manuals/om-20000062.pdf.